Molecular Crystals and Liquid Crystals
Publication details, including instructions for authors and subscription information:
http://www.tandfonline.com/loi/gmcl20

Chiral Smectics: As Observed through Dielectric Spectroscopy

M. B. Pandey [a] , R. Dhar [b] & R. Dabrowski [c]

[a] Physics Department, VSSD College, Kanpur, India

[b] Centre of Material Sciences, Institute of Interdisciplinary Studies, University of Allahabad, Allahabad, India

[c] Institute of Chemistry, Military University of Technology, Warsaw, Poland

Version of record first published: 30 Jun 2011

To cite this article: M. B. Pandey, R. Dhar & R. Dabrowski (2011): Chiral Smectics: As Observed through Dielectric Spectroscopy, Molecular Crystals and Liquid Crystals, 541:1, 222/[460]-235/[473]

To link to this article: http://dx.doi.org/10.1080/15421406.2011.569242

Mol. Cryst. Liq. Cryst., Vol. 541: pp. 222/[460]–235/[473], 2011

ISSN: 1542-1406 print/1563-5287 online
DOI: 10.1080/15421406.2011.569242

Chiral Smectics: As Observed through Dielectric Spectroscopy

M. B. PANDEY,[1] R. DHAR,[2] AND R. DABROWSKI[3]

[1]Physics Department, VSSD College, Kanpur, India
[2]Centre of Material Sciences, Institute of Interdisciplinary Studies, University of Allahabad, Allahabad, India
[3]Institute of Chemistry, Military University of Technology, Warsaw, Poland

Chiral compounds show rich variety of smectic phases viz. SmC_α^*, SmC_β^*, SmC_γ^*, SmC^*, SmC_A^* due to different correlation between adjacent layers and various TGB phases due to different orientation of blocks of layers. Dielectric spectroscopy has proven as an important tool for the characterization of various smectic phases posses by chiral compounds. Dielectric spectra of these phases are sometimes complex but rich in information and are very helpful in the determination of the structure of these phases. Dielectric spectroscopy of the above phases observed in the recently synthesized materials is discussed with regards to their structure property relationship.

Keywords Dielectric relaxation; ferroelectric and antiferroelectric phases; SmC_α^* phase; TGB phases

1. Introduction

Chiral smectic mesophases have become matter of curiosity amongst liquid crystal community due to their reduced symmetry properties which allowed spontaneous polarization in the smectic layers as well as novel structures. Dielectric properties of classical liquid crystals (nematics and smectics) are intensively studied for their technical exploitation and from the structural point of view. When ferroelectrcity in chiral smectic phase was discovered in 1975 by Meyer *et al.* [1], dielectric spectroscopy became even more important characterization technique in the field of liquid crystals research. The presence of spontaneous polarization in chiral smectic C (SmC^*) phase leads to a very interesting dielectric response as compared to a chiral liquid crystals. Latter on in 1989, when Antiferroelectric Liquid Crystals (AFLCs) with the plethora of subphases in the SmC^* family [2] and frustrated twisted grain boundary (TGB) phases were discovered [3,4], dielectric characterization became a necessity. Each chiral smectic phase has a specific dielectric response and electrical properties. Hence a dielectric spectrum may, therefore, provide very good help in

Address correspondence to R. Dhar, Centre of Material Sciences, Institute of Interdisciplinary Studies, University of Allahabad, Allahabad-211 002, India. Fax: +91-532-2466122; E-mail: dr_ravindra_dhar@hotmail.com

identifying phases of new materials. Structure and dielectric properties of several new phases are not yet completely understood. Another very appealing characteristic of dielectric spectroscopy is that it works equally for thin and thick samples. This makes it an ideal technique to study how the surfaces affect the phase behaviour and phase sequence of a material. Also the complete alignment of the sample, with some exception is not so crucial for the results. Therefore, dielectric spectroscopy is a very good complement to techniques which are more sensitive to the alignment conditions. In this article, a comprehensive report of dielectric relaxation processes of various smectic phases (viz. SmC_α^*, SmC^*, SmC_β^*, SmC_γ^* and SmC_A^*) and TGB phases (viz. TGBA, TGBC and TGBC*) of LC materials are discussed with regard to structure of the phases.

2. Experimental

For the study of the dielectric properties of chiral smectic systems, the measuring cell is taken in the form of parallel plate capacitor made from ITO or gold coated conducting glass electrodes and separated by mylar/teflon spacers of known thickness. The planar and homeotropic orientations of the molecules are obtained by chemically treating the glass plates [5]. As the liquid crystals are anisotropic media ($\triangle\varepsilon' = \varepsilon'_{||} - \varepsilon'_{\perp} \neq 0$), different results are obtained for different alignments of the sample. When measuring field is directed perpendicular to the plane of cell, one should in principle measure $\varepsilon'_{||}$ in the homeotropic alignment and $\varepsilon'_{\perp}$ in the planar alignment. However, it must be kept in mind that no cell is perfectly aligned and a non-zero tilt or presence of helix (especially in chiral phases) will of course also lead to an effective mixture of director orientation throughout the cell. Therefore, in many cases, we may observe a combination of $\varepsilon'_{||}$ and $\varepsilon'_{\perp}$ in the same measurement. Even though the effect normally is small, it may sometimes play an important role. In our work, Impedance/Gain-phase analyzer of Solartron (model SI-1260) coupled with Solartron dielectric interface (model-1296) has been used to acquire the dielectric data. Most of the measurements are restricted to the frequency range of 1 Hz to 10 MHz due to the dominating electrode polarization effect below 1 kHz [5] and high frequency effect due to finite surface resistance of glass electrodes and lead inductance above 1 MHz [6,7].

To analyse the measured data, the dielectric spectra have been fitted with the help of generalized Havriliak and Negami (HN) equation [8–10]:

$$\varepsilon^* = \varepsilon' - j\varepsilon'' = \varepsilon'(\infty) + \sum_i \frac{\Delta\varepsilon_i}{\left[1 + (j\omega\tau_i)^{(1-h_i)}\right]^{\beta_i}} + \frac{A}{\omega^n} + \frac{\sigma_{ion}}{j\varepsilon_0\omega} - jB\omega^m \qquad (1)$$

where $\Delta\varepsilon_i = \varepsilon'(0) - \varepsilon'(\infty)$, τ_i and h_i are the dielectric strength, the relaxation time and the symmetric distribution parameter ($0 \leq h_i \leq 1$) of ith mode, respectively. $\varepsilon'(0)$ and $\varepsilon'(\infty)$ are the low and high frequency limiting values of the relative dielectric permittivity. β_i is asymmetric distribution parameter. The third and fourth terms in Eq. (1) are added due to the presence of electrode polarization capacitance and ionic conductance at low frequencies [5], where A and n are fitting constants [5]. σ_{ion} is the ionic conductance and $\varepsilon_0 = 8.85$ pF/m is the free space permittivity. The fifth imaginary term $B\omega^m$ is added in Eq. (1) to partially account for high frequency ITO effect [7], where B and m are constants as for as correction terms are small [6,7].

3. Results and Discussion

The chiral smectic phases can be classified in three broad categories viz. Ferroelectric Liquid Crystals (FLCs), Antiferroelectric Liquid Crystals (AFLCs) along with the associated subphases and Twisted Grain Boundary (TGB) phases. In the following sub-sections, we will discuss collective relaxation processes observed for planar orientation of the sample in the aforesaid phases.

3.1. *Molecular Dynamics of SmA* and SmC* Phases*

FLCs are classical chiral systems which show a transition from orthogonal SmA* or chiral nematic to tilted SmC* phase. Their dielectric behaviours are most studied and well established [10–12]. In the SmA* phase, the dielectric spectrum contains single relaxation mode in the high kHz region for which dielectric strength increases and corresponding relaxation frequency decreases with decrease in the temperature. Near SmA*-SmC* transition, the behaviour of this mode becomes critical. This phenomenon has been linked to the amplitude fluctuations of the tilt angle. The elastic constant controlling the tilt fluctuations gets soft on approaching SmA*-SmC* transition temperature on cooling, consequently fluctuation amplitude increases drastically and its susceptibility diverges. Thus this mode has been assigned as soft mode [10–12].

In the SmC* phase, a mode with low frequency ($\sim$1 kHz) and high strength is generally observed for planar orientation of the sample. This mode could be suppressed by application of bias electric field. The SmC* phase is characterized by chirality, molecular tilt and the helical structures. The director makes an angle with the smectic layer normal and it precesses with a finite phase angle (φ) from one layer to another resulting in a helical structure with helical axis parallel to the normal to the smectic layer [10–12]. When a small measuring electric field is applied across the sample, a mode is observed due to the distortion of phase angle which propagate along the helical axis. This type of fluctuation manifests itself as a distortion of phase angle and is called Goldstone mode. Soft mode is also present in the SmC* phase but it is generally masked by strong Goldstone mode. It could be observed after suppressing Goldstone mode by applying bias electric field [8,10–12].

3.2. *Molecular Dynamics of SmC_A^* Phase*

In the SmC_A^* phase, two relaxation modes are observed under planar anchoring of the molecules by dielectric spectroscopy (see Fig. 1). The behaviour of the corresponding relaxation frequencies depends on the adjacent high temperature phase in the material [13–28]. Relaxation frequencies of these modes show dependence with temperature whereas corresponding dielectric strength are very small ($\sim$1) and remains almost invariant with temperature [17–19]. These two modes generally show Arrhenius type behaviour. However, their frequency ranges and slopes are different (see Fig. 2) as compared to that of the mode corresponding to the reorientation of molecules around their short axis [24–26]. The relaxation frequencies of these two modes are found to be invariant with bias electric field and thickness of the sample [18,26]. However, dielectric strength of these modes increase with increase in the bias electric field and support the hypothesis of their collective nature (see Fig. 3) [14,18,19]. The low frequency mode of SmC_A^* phase has features typical of a

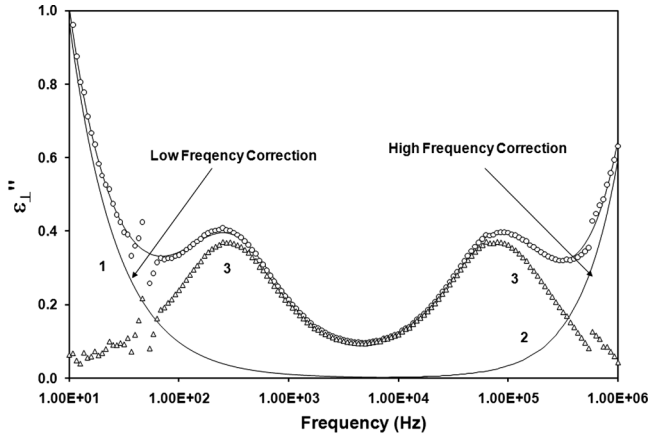

(a)

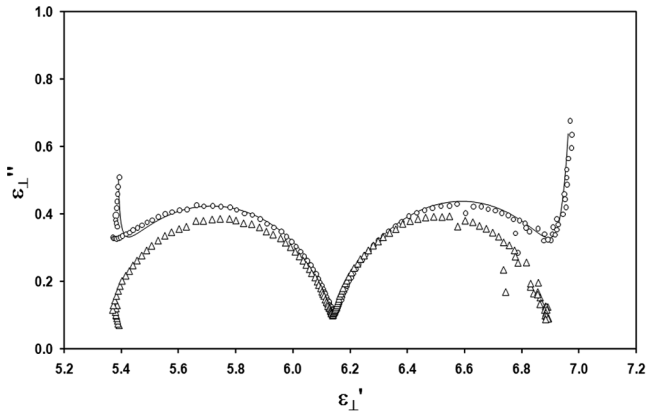

(b)

Figure 1. (a) Variation of dielectric loss of Cl-MHPOBC at 31.8°C. An example of mode separation by simulation of experimental data (open symbol) using Eq. (1). (b) Cole-Cole plots in the SmC_A^* phase of Cl-MHPOBC at 27.7°C. The experimental data and corrected data are shown by open circles and triangles respectively.

Goldstone mode. It is well known that, a helicoidal superstructure exist in SmC_A^* phase, with anti-tilt pair spiraling in a certain direction. The molecular directors in the adjacent smectic layers of SmC_A^* phase are not completely anti-parallel to each other, so there is slight imbalance in the local polarization. This causes 'the antiferroelectric spontaneous polarization' δP. Such an 'antiferroelectric polarization' spirals about the helical axis as does the polarization in ferroelectric (SmC^*) phase. Hence one can expect the dielectric relaxation process to arise from the distortion of the antiferroelectric helix due to interaction of measuring ac electric field with δP similar to that of a ferroelectric Goldstone mode, though with a low value of the dielectric strength [17–19]. The high frequency mode has been considered to originate from the fluctuation of the directors in the anti-tilt pairs of the SmC_A^* phase where they rotate in opposite phase, hence is called anti-phase azimuthal angle fluctuation mode [14,17–19].

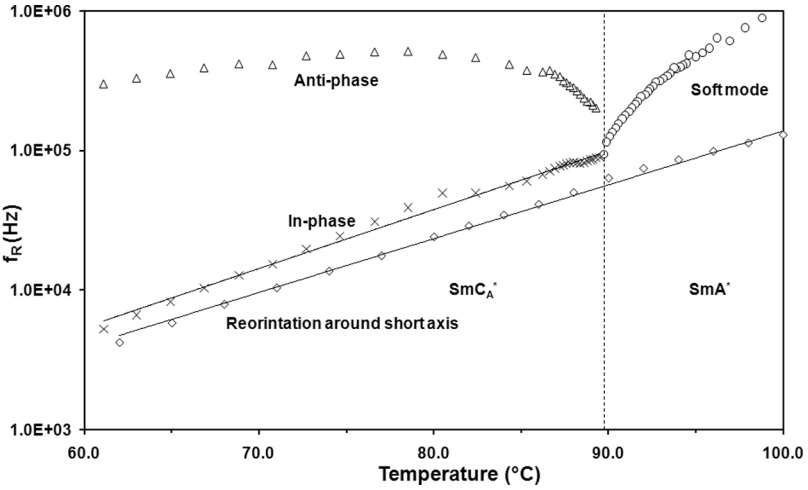

Figure 2. Temperature dependence of the relaxation frequencies of three observed modes in-phase and anti-phase (in planar alignment) and reorientation around short axis (quasi-homeotropic alignment) in the SmC_A^* phase of MHPB(H)PBC.

3.3. *Molecular Dynamics of Chiral Smectic C (SmC_α^*, SmC_β^* and SmC_γ^*) sub-phases*

In the dielectric spectrum of the SmC_α^* phase, most often one collective relaxation process is observed that exist in the high kHz region [13,15–17]. Origin of this mode is assigned to tilt fluctuation of molecules i.e., soft mode. In some materials a collective mode in low kHz region is also reported and its origin has been assigned to Goldstone mode [8,16]. In one of the material (S)-(+)-4-(1-methylheptyl) 4-[4-(3--hexanoyloxy) prop-1-oxy) benzoyloxy] biphenylate studied by us which shows

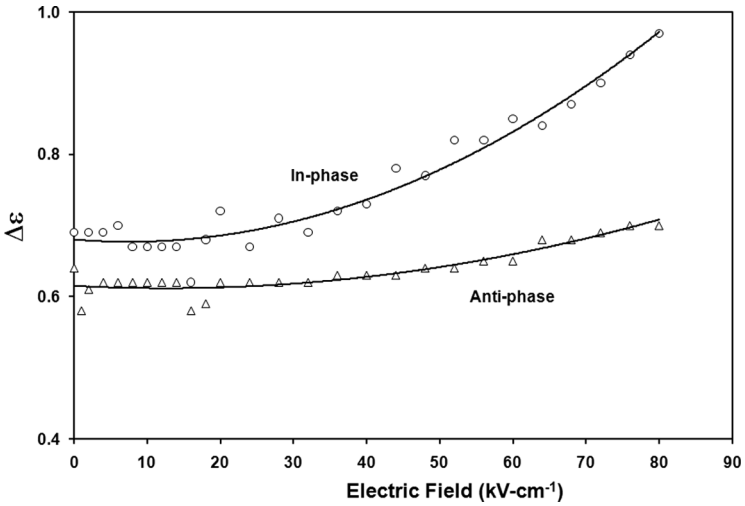

Figure 3. Bias field dependence of the dielectric strength of two modes (in-phase and anti-phase) of the SmC_A^* phase of Cl-MHPOBC at 39.8°C for the planar aligned sample.

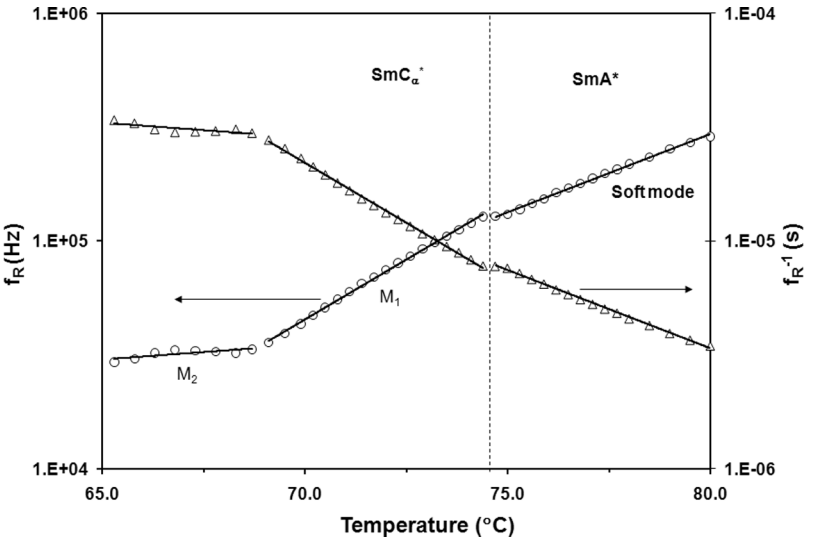

Figure 4. Variation of relaxation frequencies (f_R) and their inverse (f_R^{-1}) with temperature in SmA* and SmC_α^* phases of (S)-(+)-4-(1-methylheptyl) 4-[4-(3-hexanoyloxy) prop-1-oxy) benzoyloxy] biphenylate.

SmC_α^* phase in wide temperature range (~9°C), two different behaviour of relaxation processes have been observed in different temperature range as shown in Figures 4 and 5 [29,30]. On the basis of temperature, frequency and bias electric field dependent studies of dielectric parameters, we have confirmed that the collective

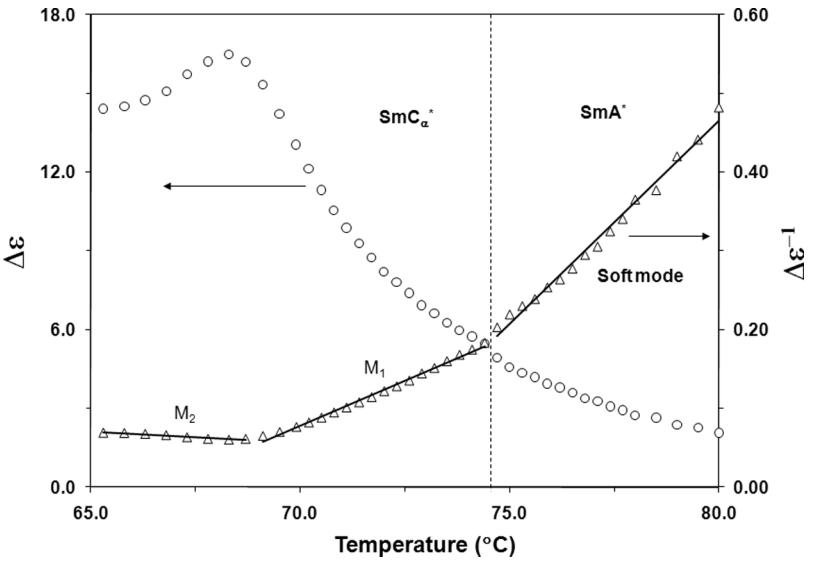

Figure 5. Variation of dielectric strength ($\triangle\varepsilon$) and their inverse ($\triangle\varepsilon^{-1}$) with temperature in SmA* and SmC_α^* phases of (S)-(+)-4-(1-methylheptyl) 4-[4-(3-hexanoyloxy) prop-1-oxy) benzoyloxy] biphenylate.

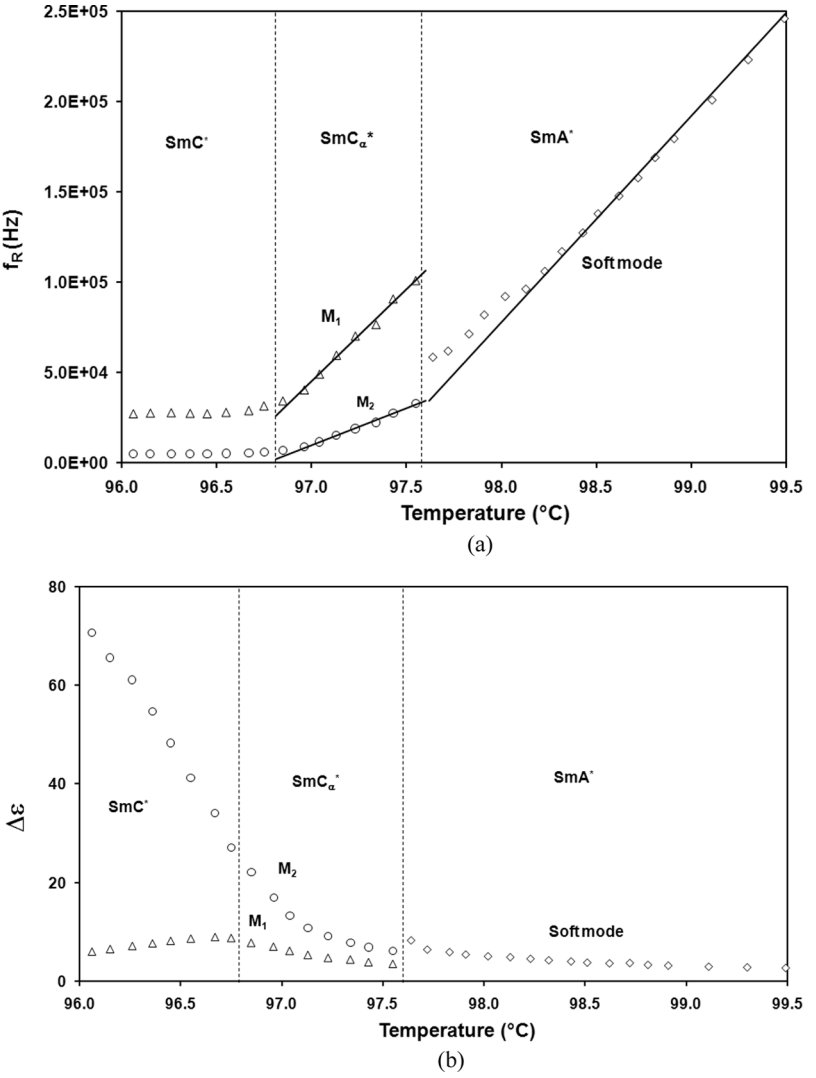

Figure 6. Temperature dependence of (a) relaxation frequency (f_R) and (b)dielectric strength ($\triangle\epsilon$) of various modes of SmA*, SmC$_\alpha$* and SmC* phases of Cl-MHPOBC in the cooling cycle.

dielectric relaxation mode of SmC$_\alpha$* phase behaves like soft mode near SmA*-SmC$_\alpha$* transition. However, far from the transition, it behaves as phase fluctuation (Goldstone like) mode. A theoretical model is proposed by Vaupotic *et al.* which predicts amplitude and phase fluctuation modes in SmC$_\alpha$* phase simultaneously [31]. We have verified this assumption in a compound Cl-MHPOBC where two relaxation modes (M_1 and M_2) are observed simultaneously as shown in Figure 6 [8]. The high frequency mode (M_1) possesses small dielectric strength (~4–8) and its frequency varies between 100 kHz and 32 kHz. The low frequency mode (M_2) is observed between 40 kHz and 8 kHz and possesses high dielectric strength. The dielectric

strength of the low frequency mode decreases with increase in bias electric field and is suppressed at a critical value of 36 kV-cm^{-1} [8]. It is important to mention here that due to short helical pitch of SmC_α^* phase (<100 nm), Goldstone mode is expected with small strength but at higher frequency (than usually observed in the SmC^* phase), which may be of the order of the frequency of the soft mode. Hence these two modes are superimposed to each other in the dielectric spectrum.

The SmC_β^* is considered to be antiferroelectric with modulation of four smectic layers in a unit cell [13]. Hence the two observed relaxation processes in this phase have generally similar nature as discussed for the SmC_A^* phase. In the SmC_γ^* phase, two modes are observed in low (~1 kHz) and high (~100 kHz) kHz regions respectively [13–17,20,21]. The temperature dependences of the relaxation frequencies and dielectric strengths of various modes are shown in Figures 7a and 7b respectively for a compound (S)-(+)-4′-[4-(1-methylheptyloxycarbonyl)] biphenyl 4-[3-(octanoyloxy) prop-1-oxy]benzoate [32]. The relaxation frequency and dielectric strength of low frequency mode (marked M_3 in Fig. 7) decreases with decrease in temperature. The decrease of dielectric strength of low frequency mode in SmC_γ^* phase, occurs due to the decrease in ferroelectric order (or increase in antiferroelectric order) with decrease in the temperature. The dielectric strength and relaxation frequency of high frequency relaxation mode (M_4) remains almost invariant with temperature. This reminds typical behaviour of a mode observed in high kHz region in the antiferroelectric SmC_A^* phase (as discussed in previous paragraph). It may be presumed that high frequency relaxation mode appears due to presence of partial antiferroelectric ordering in SmC_γ^* phase. It is observed that low frequency mode vanishes near SmC_γ^*-SmC_A^* phase transition. On the basis of temperature dependence, low frequency mode of SmC_γ^* phase are stipulated due to ferrielectric Goldstone and high frequency mode is due to anti-phase azimuthal angle fluctuations respectively.

3.4 *Molecular Dynamics of TGB Phases*

Static dielectric measurement is proven to be a tool for the determination of weak transitions especially in TGB systems which could not be observed by thermal scanning measurement [33–36]. Variations of $\varepsilon'_{||}$ and $\varepsilon'_{\perp}$ with temperature showing dielectric anisotropy ($\delta\varepsilon'$) is shown in Figure 8 for the binary mixture of HOAB and ChB [35]. N^*-$TGBC^*$ transition is clearly visible by change in pattern for both components of the permittivity. Static dielectric measurement also gives information about structure of the phases. As $\delta\varepsilon'$ in $TGBC^*$ phase is approximately zero, hence, it can be presumed that molecular orientation are similar in $TGBC^*$ phase for two cases of anchoring. Similar results are also found in a series of compounds (DC4–10 and 11) [33]. This indicates cubic structure of $TGBC^*$ phase. One must keep in mind that $TGBC^*$ phase has additional helix (of the SmC^* structure inside the smectic blocks) normal to the usual TGB helix similar to those in TGBA and TGBC phases [4].

Initial dynamic dielectric studies of the TGBA phase carried out by other groups [37–41] show that, like those of SmA^* phase, electric field induces amplitude fluctuation of tilt angle i.e., soft mode. Similarly in TGBC phase, electric field induces phase fluctuation of the tilt angle and hence Goldstone like mode of dielectric relaxation is observed as it is in the SmC^* phase [39,40]. However, experimental evidences suggest that relaxation processes of TGB phases have small amplitudes and higher relaxation frequencies as compared to those observed in classical SmA^* and SmC^* phases. Ismaili *et al.* [40] have proposed a theoretical model verified by

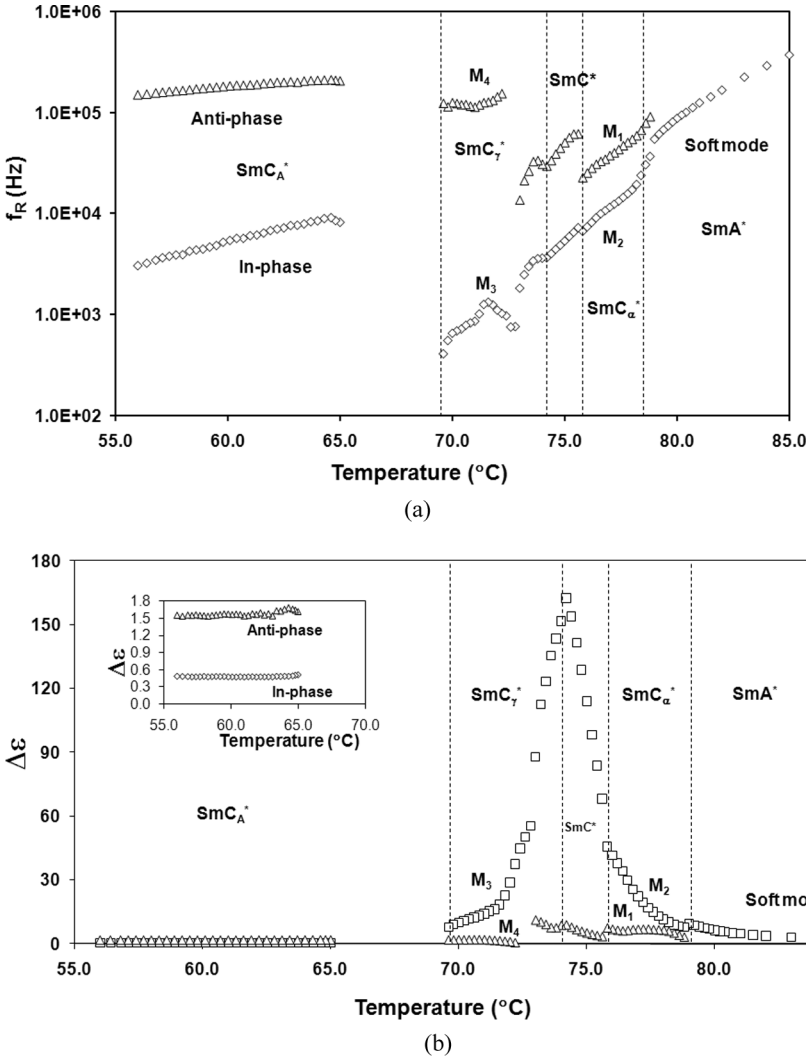

Figure 7. Temperature dependence of (a) relaxation frequencies (f_R) and (b) dielectric strengths of various modes observed in different phases of (S)-(+)-4′-[4--(1-methylheptyloxycarbonyl)] biphenyl 4-[3-(octanoyloxy) prop-1-oxy]benzoate. Two modes of SmC_α^* (M_1 and M_2) and SmC_γ^* (M3 and M4) phases are distinctively visible here.

some experimental work, which suggests that Goldstone mode of TGBC and soft mode of TGBA phases are strongly reduced due to the elastic distortion of the director which depends on anchoring forces at the grain boundaries and distance between them. Dielectric studies of a wide temperature range TGBA phase (~31°C) in a binary mixture of 7OCB and 5*CBB is earlier reported [42]. Relaxation frequency of observed mode in the TGBA phase lies in the range of 200 kHz to 2 MHz and its dielectric strength varies from 0.42 to 0.18 [42]. Novotna *et al.* have reported the soft and Goldstone modes in the TGBA and TGBC* phases of a series HZL/* which have very high strength probably due to the low temperature SmC* phase [43].

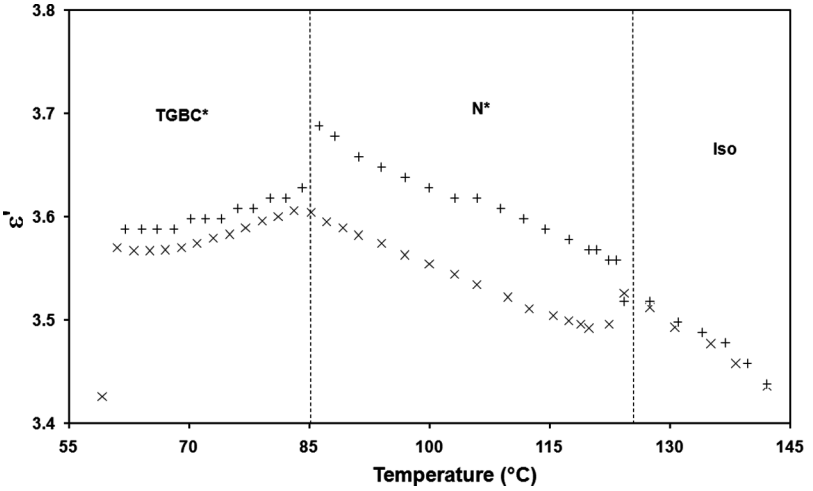

Figure 8. Variations of $\varepsilon'_{||}$ (cross) and $\varepsilon'_{\perp}$ (plus) in the mixture of HOAB (82 wt%) and ChB (18 wt%) at 100 kHz reflecting dielectric anisotropy ($\delta\varepsilon'$) with temperature. Low frequency data (1 kHz) after the removal of the low frequency parasitic effect have been taken as the static dielectric permittivity.

In the antiferroelectric $TGBC_A^*$ phase, a relaxation mode in the kHz region has been reported by Petrenko *et al.* in a compound (S)-1-Methylheptyl 2-[4-(4-dodecyloxybenzoyloxy)phenyl]-pyrimidine-5-carboxylate [44]. Relaxation frequency and corresponding dielectric strength of this mode does not change with temperature, yet this mode is attributed to the soft mode [44].

Static dielectric permittivity is also important to detect weak and broad relaxation processes where it is not possible to get correct value of strength by the direct or fitting process [45–48]. The temperature dependence of $\varepsilon'_{\perp}$ at various frequencies is shown in Figure 9 for a compound DC 4–11 which shows only TGBA and TGBC* phases [45]. Two weak transitions in the compound can be clearly seen in Figure 9. The value of $\varepsilon'_{\perp}$ is almost invariant with frequency in the isotropic liquid phase implying that no molecular relaxation exists in this phase over the experimental frequency range. On lowering the temperature, in the TGBA phase (below ~119°C), $\varepsilon'_{\perp}$ shows some decrease for the frequencies above 100 kHz, indicating a pre dielectric dispersion phenomenon in the frequency range of 100 kHz to 1 MHz. As temperature goes down, this mechanism further dominates. From Figure 9, one can see that, while going from 10 kHz to 1 MHz, $\varepsilon'_{\perp}$ decreases by ~0.2 (at 111°C). On the basis of the range of the relaxation frequency and its strength, this weak relaxation mode is assigned to soft mode of TGBA phase [45]. At TGBA-TGBC* transition, low frequency values (10 Hz-100 Hz) of $\varepsilon'_{\perp}$ further go up however high frequency values of $\varepsilon'_{\perp}$ move down (see Fig. 9). It is apparent from these dielectric data that soft mode of TGBA phase continues in TGBC* phase as well, with increase in its strength. In the low frequency region (<1 kHz) of TGBC* phase, $\varepsilon'_{\perp}$ increases upon decreasing temperature. This indicates the presence of another collective relaxation mechanism in TGBC* phase between 1 kHz to 10 Hz; however data below 100 Hz are highly affected due to low frequency parasitic contributions. After subtracting the low frequency artifacts from the measured data, a mode below 1 kHz is clearly visible in the

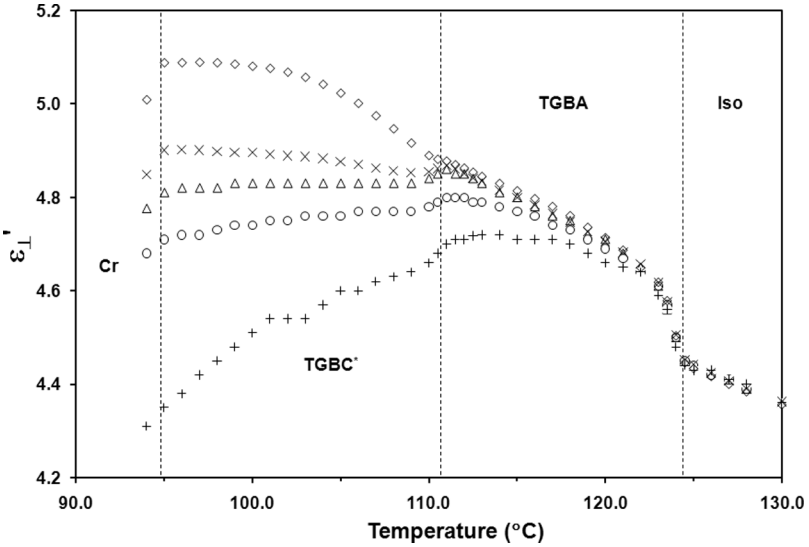

Figure 9. Variation of $\varepsilon'_{\perp}$ with temperature at 100 Hz (square), 1 kHz (cross), 10 kHz (triangle), 100 kHz (circle) and 1 MHz (plus) for compound DC4-11.

TGBC* phase as shown in Figure 10 [46]. On the basis of its frequency range and other dielectric parameters, this process is assigned to Goldstone like mode of the TGBC* phase [46]. Small value of the transverse component of the molecular dipole moment may be the reason for the weak dielectric strength of the observed mode in TGB systems. We here stress that any firm evidence has yet not been found to relate

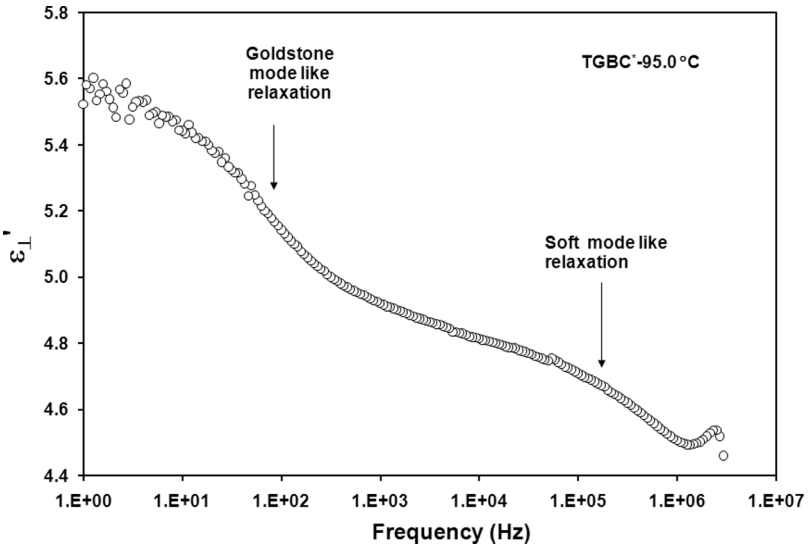

Figure 10. Variation of $\varepsilon'_{\perp}$ (corrected after removing low and high frequency parasitic effects) with frequency at 95°C in the TGBC* phase of DC4-11.

observed modes of TGB systems to tilt and phase angle fluctuations; nevertheless the above hypothesis still remain the most likely explanation. However, a most interesting system yet to be explored would be one having phase sequence: N*-TGBA-TGBC-TGBC*-SmC* with large value of the transverse component of dielectric permittivity. Such a system may give conclusive evidence of the expected modes of the TGB phases. Presence of all the above phases in a material will make various parameters of different phases distinctively comparable.

4. Conclusions and Perspectives

Dielectric spectroscopy has proven to be an effective tool in the identification of chiral smectic phases and their structural properties as discussed above. Two relaxation modes detected simultaneously, in the SmC_{α}^{*} phase, have shown their characteristics as soft mode and Goldstone mode in concurrence with the proposed theoretical model. Similarly, modes detected in the SmC_{β}^{*} and SmC_{γ}^{*} phases confirms their antiferroelectric and ferrielectric behavior, respectively. Soft and Goldstone modes like relaxations have been detected in the TGBA and TGBC phases as theoretically expected. However, presence of the two helix axes in the TGBC* phase (there is additional helix of the SmC* structure in the smectic blocks and it is normal to the usual TGB helix), makes it complex. Consistent experimental data and theoretical approach are required to draw any conclusion about the origin of the relaxation processes in this phase.

Acknowledgement

Financial supports from the Department of Science and Technology (DST), New-Delhi and the University Grants Commission (UGC), New Delhi are thankfully acknowledged.

References

[1] Meyer, R. B., Liebert, L., Strzelecki, L., & Keller, P. (1975). *J. Phys. (Paris) Let.*, *36*, 69.
[2] (a) Chandani, A. D. L., Ouchi, Y., Takezoe, H., Fukuda, A., Terashima, K., Furukawa, K., & Kishi, A. (1989). *Jpn. J. Appl. Phys.*, *28*, L1261; (b) Galerne, Y., & Liebert, L. (1991). *Phys Rev. Lett.*, *66*, 2891.
[3] Goodby, J. W., Waugh, M. A., Stein, S. M., Chin, E., Pindak, R., & Patel, J. S. (1989). *Nature*, *337*, 449.
[4] (a) Renn, S. R., & Lubensky, T. C. (1991). *Mol. Cryst. Liq. Cryst.*, *209*, 349; (b) Renn, S. R. (1992). *Phys. Rev. A*, *45*, 953.
[5] Srivastava, S. L., & Dhar, R. (1991). *Indian J. Pure Appl. Phys.*, *29*, 745.
[6] (a) Srivastava, S. L. (1993). *Proc. Nat. Acad. Sci. India*, *63*, 311; (b) Dhar, R. (2004). *Ind. J. Pure Appl. Phys.*, *42*, 56.
[7] Gouda, F. M., Skarp, K., & Lagerwall, S. T. (1991). *Ferroelectrics*, *113*, 165.
[8] Hill, N. E. (1969). Theoretical treatment of Permittivity and Loss. In Hill, N. E., Vaughan, W. E., Price, A. H., & Davies, M. (Eds.), Chapter 1, p. 1 Van Nostrand Reinhold Co: London.
[9] Pandey, M. B., Dhar, R., Agrawal, V. K., Khare, R. P., & Dabrowski, R. (2003). *Phase Transitions*, *76*, 945.
[10] Pandey, M. B., Dhar, R., Agrawal, V. K., & Dabrowski, R. (2004). *Mol. Cryst. Liq. Cryst.*, *414*, 63.

[11] Pandey, M. B., Dhar, R., & Dabrowski, R. (2008). *Liq. Cryst.*, *35*, 777.
[12] Levstik, A., Carlsson, T., Filipic, C., Levstik, I., & Zeks, B. (1987). *Phys. Rev. A*, *35*, 3527.
[13] Fukuda, A., Takanishi, Y., Isozaki, T., Ishikawa, K., & Takezoe, H. (1994). *J. Mater. Chem.*, *4*, 997.
[14] Buivydas, M., Gouda, F., Lagerwall, S. T., & Stebler, B. (1995). *Liq. Cryst.*, *18*, 879.
[15] Merino, S., Fuente, M. R. de la, Gonzalez, Y., Perez Jubindo, M. A., Ros, B., & Puertolas, J. A. (1996). *Phys. Rev. E*, *54*, 5169.
[16] Hou, J., Schacht, J, Gießelmann, F., & Zugenmaier, P. (1997). *Liq. Cryst.*, *22*, 409.
[17] Pandey, M. B., Dhar, R., Agrawal, V. K., Dabrowski, R., & Tykarska, M. (2004). *Liq. Cryst.*, *31*, 973.
[18] Pandey, M. B., Dabrowski, R., & Dhar, R. (2007). *Physica B*, *287*, 25.
[19] Pandey, M. B., Dhar, R., & Dabrowski, R. (2008). *Philosophical Magazine*, *88*, 101.
[20] Buivydas, M., Gouda, F., Andersson, G., Lagerwall, S. T., Stebler, B., Bomelburg, J., Heppke, G., & Gestblom, B. (1997). *Liq. Cryst.*, *23*, 723.
[21] Panarin, Y. P., Kalinovskaya, O., & Vij, J. K. (1998). *Liq. Cryst.*, *25*, 241.
[22] Marzec, M., Mikulko, A., Wrobel, S., Haase, W., & Dabrowski, R. (2005). *Mol. Cryst. Liq. Cryst.*, *437*, 169.
[23] Rudquist, P., Lagerwall, J. P. F., Meier, J. G., D'have, K., & Lagerwall, S. T. (2002). *Phys. Rev. E.*, *66*, 061708.
[24] Pandey, M. B., Dhar, R., Agrawal, V. K., & Dabrowski, R. (2005). *Phase Transitions*, *78*, 57.
[25] Pandey, M. B., Dhar, R., & Dabrowski, R. (2006). *Ferroelectrics*, *343*, 83.
[26] Pandey, M. B., Dhar, R., & Dabrowski, R. (2006). *mySCIENCE*, University of Mysore, India, *1* (2), 135.
[27] Dwivedi, A., Dhar, R., Pandey, M. B., Das, I. M. L., & Dabrowski, R. (2009). *Mol. Liq.*, *148*, 01.
[28] Kumari, S., Dhar, R., Pandey, M. B., Das, I. M. L., & Dabrowski, R. (2009). *J. Phys. Chem. Solids*, *70*, 316.
[29] Pandey, M. B., Dhar, R., & Dabrowski, R. (2008). *Journal of Physics: Condensed Matter*, *20*, 115207.
[30] Pandey, M. B., Dhar, R., & Dabrowski, R. (2009). *Mol. Cryst. Liq. Cryst.*, *509*, 363.
[31] Vaupotic, N., Cepic, M., & Zeks, B. (2000). *Ferroelectrics*, *245*, 175.
[32] Pandey, M. B., Dabrowski, R., & Dhar, R. (2010). *Ferroelectrics*, *395*, 99.
[33] Pandey, M. B., & Dhar, R. (2009). *Journal of the Indian Institute of Science*, *89* (2), 147.
[34] Dhar, R., Pandey, M. B., & Agrawal, V. K. (2003). *Phase Transitions*, *76*, 763.
[35] Pandey, M. B., Dhar, R., & Kuczynski, W. (2006). *Ferroelectrics*, *343*, 69.
[36] Otowski, W. (2007). In *Molecular Motion in Liquid Crystals as Seen Via Dielectric Spectroscopy*, Galewski, Z., & Sobczyk, L. (Eds.), Chapter 1, p. 1, Transworld Research Network: Trivandrum, India.
[37] Wrobel, S., Hiller, S., Pfeiffer, M., Marzec, M., & Haase, W. (1995). *Liq. Cryst.*, *18*, 21.
[38] Xu, H., Panarin, Y. P., Vij, J. K., Seed, A. J., Hird, M., & Goodby, J. W. (1995). *J. Phys.: Cond. Matter*, *7*, 7443.
[39] Bougrioua, F., Isaert, N., Legrand, C., Bouchta, A., Barois, P., & Nguyen, H. T. (1996). *Ferroelectrics*, *180*, 35.
[40] Ismaili, M., Bougrioua, F., Isaert, N., Legrand, C., & Nguyen, H. T. (2001). *Phys. Rev. E*, *65*, 011701.
[41] Dodge, M. R., Vij, J. K., Cowling, S. J., Hall, A. W., & Goodby, J. W. (2005). *Liq. Cryst*, *32*, 1045.
[42] Gupta, M., Dhar, R., Agrawal, V. K., Dabrowski, R., & Tykarska, M. (2005). *Phys. Rev. E*, *72*, 021703.
[43] Novotna, V., Kaspar, M., Hamplova, V., Glogarova, M., Bilkova, P., Domenici, V., & Pociecha, D. (2008). *Liq.Cryst.*, *35*, 287.

[44] Petrenko, A. S., Hird, M., Lewis, R. A., Meier, J., Jones, J. C., & Goodby, J. W. (2000). *J. Phys: Condensed Matter*, *12*, 8577.
[45] Pandey, M. B., Dhar, R., Achalkumar, A. S., & Yelamaggad, C. V. (2007). *J. Phys: Condensed Matter*, *19*, 436219.
[46] Pandey, M. B., Dhar, R., Achalkumar, A. S., & Yelamaggad, C. V. (2008). *Phase Transitions*, *81*, 449.
[47] Pandey, A. S., Dhar, R., Pandey, M. B., Achalkumar, A. S., & Yelamaggad, C. V. (2009). *Liq. Cryst.*, *36*, 13.
[48] Dhar, R., Pandey, M. B., Pandey, V. S., Pandey, A. S., Das, I. M. L., Achalkumar, A. S., & Yelamaggad, C. V. (2009). *Opto-electronics Reviews*, *17* (2), 144.